DOI: 10.3901/CJME.2013.05.861, available online at www.springerlink.com; www.cjmenet.com; www.cjmenet.com.cn

Effects of Joint on Dynamics of Space Deployable Structure

GUO Hongwei*, ZHANG Jing, LIU Rongqiang, and DENG Zongquan

School of Mechanical and Electrical Engineering, Harbin Institute of Technology, Harbin 150001, China

Received August 30, 2012; revised March 28, 2013; accepted April 3, 2013

Abstract: Joints are necessary components in large space deployable truss structures which have significant effects on dynamic behavior of these joint dominated structures. Previous researches usually analyzed effects of one or fewer joint characters on dynamics of jointed structures. Effects of joint stiffness, damping, location, number, clearance and contact stiffness on dynamics of jointed structures are systematically analyzed. Cantilever beam model containing linear joints is developed based on finite element method, influence of joint on natural frequencies and mode shapes of the jointed system are analyzed. Analytical results show that frequencies of jointed system decrease dramatically when peak mode shapes occur at joint locations, and there are cusp shapes present in mode shapes. System frequencies increase with joint damping increasing, there are different joint damping to achieve maximum system damping for different joint stiffness. Joint nonlinear force-displacement is described by describing function method, one-DOF model containing nonlinear joints is established to analyze joints freeplay and hysteresis nonlinearities. Analysis results show that nonlinear effects of freeplay and hysteresis make dynamic responses switch from one resonance frequency to another frequency when amplitude exceed demarcation values. Joint contact stiffness determine degree of system nonlinearity, while exciting force level, clearance and slipping force affect amplitude of dynamic response. Dynamic responses of joint dominated deployable truss structure under different sinusoidal exciting force levels are tested. The test results show obvious nonlinear behaviors contributed by joints, dynamic response shifts to lower frequency and higher amplitude as exciting force increasing. The test results are further compared with analytical results, and joint nonlinearity tested is coincident with hysteresis nonlinearity. Analysis method of joint effects on dynamic characteristics of jointed system is proposed, which can be used in optimal design of joint parameters to achieve optimum dynamic performance of jointed system.

Key words: deployable structure, joint, dynamic, mode shape, experiment

1 Introduction

Space deployable structures play a significant role in various space exploration activities, e.g., high resolution earth observation, deep space exploration and satellite communication. They are widely used to deploy and support space instruments such as flexible solar array, antenna, synthetic aperture radar, space telescope due to they can be folded into very small volumes during launch process[1–2]. Joints or hinges are usually necessary components in the space deployable strcutures. Numerous joints or hinges are used to connect link elements or modules to achieve higher packaging efficiency, larger scale and less weight. These joints or hinges can affect dynamics, stability and precision of the jointed space structures. The joints are commonly known to be the main resource of the nonlinearities and damping to the system, and joints usually make the system more flexible[3]. So how the joints affect the stiffness, damping, vibration mode shapes and dynamic responses of the system must be studied carefully, and dynamic model considering joints must be accurately modelled to meet mission requirements.

Due to the large jointed deployable structures are widely used in space, mechanic characteristics of joint have been investigated by numerous of researchers[4–6]. The finite element method, experiment method and analytical method were used to study the influence of joint on dynamics or accuracy of jointed deployable structures. For example, DUTSON, et al[7], developed a model of a single strut which considering friction, impacting, and damping in the joints, then this model was extended to analyze the influence of joint damping and dynamic behavior of pin-jointed truss structures. CRAWLEY, et al[8], proposed an experimental technique of force state mapping to identify and quantify the potential nonlinear dynamic properties of joint, the advantages of this technique were abilities to handle arbitrarily strong nonlinearities and plot graphical form of the data presentation directly. Later MASTERS, et al[9], extend force state mapping to the characterization of realistic multiple degree-of-freedom

* Corresponding author. E-mail: guohw@hit.edu.cn
This project is supported by National Natural Science Foundation of China(Grant Nos. 50935002, 11002039), and Postdoctoral Science Foundation of China(Grant No. 2012T50340)

(DOF) systems. BOWDEN[10] and WEBSTER, et al[11], used describing function method to model nonlinear joints in multi-DOF structures, which validated that describing function was an effective method to describe the nonlinearity of the joints. LI, et al[12], proposed a virtual experimental modal analysis method to analyze the dynamic characteristics of the deployable space structures considering joint clearance and link flexibility. TAN, et al[13], developed a nonlinear dynamic model of cable stiffened deployable structures considering effects of joint preload and passive cable pretension, analyzed the joint nonlinear dynamic characteristics under preload. STOHLMAN, et al[14], studied accuracy of a joint-dominated deployable mast, and proposed a strategy to model nonlinear joint. STOHLMAN, et al[15], also investigated effects of component properties on the accuracy of joint domninated deployable mast and shown that joint friction was an important property to affect mast accuracy. Provious research work usually focused on effects of one or fewer joint characters on dynamics of jointed structures, such as clearance, damping, however joint location and number affect jointed system significantly. BOWDEN analyzed effects of joint stiffness and damping on dynamics of beam with free-free end conditions, however dynamic characteristics of the unconstrained jointed beam were different from dynamics of deployable structures used as cantilevered beams on orbit.

In this paper, cantilever beam model containing linear joints and one DOF system model containing nonlinear joint are established respectively. These two dynamic models are used to investigate the effects of joint on dynamics of jointed structures. Effects of joint stiffness and damping on the frequencies and mode shapes of the jointed cantilever beam are analyzed and plotted in charts. Describing function method is used to describe joint nonlinear force-displacement relationship, and influence of joint nonlinearities on dynamic response of the jointed system is also analyzed systematically. Dynamic responses of a jointed deployable truss mast are tested to investigate the nonlinearities contributed by the joints. The layout of this article is as follows. Firstly, the typical jointed space deployable structures are introduced. Secondly, the linear effects of joint stiffness and damping on natural frequencies and mode shapes of jointed system are investigated. Then the nonlinear effects of different joint nonlinearities on dynamic responses of jointed system are studied. Followingly, nonlinear dynamic responses of the joint dominated deployable truss structure are tested and joint nonlinearity is identified. At last concludes the paper.

2 Jointed Space Deployable Structures

Various articulated deployable structures have already been used in several spacial missions, e.g., earth observation, deep space exploration and satellite communication for tens of years. For instance, the mobile servicing system(MSS) which is better known as the Canadarm-2 robotic arm in the international space station(ISS), as shown in Fig. 1, it is a typical articulated boom[16]. It is fully deployment length is 17.6 m long, and has seven motorised joints, each giving one degree of freedom.

Fig. 1. Mobile servicing system

Space deployable truss structure is another kind of articulated deployable structure containing a number of pinned joints or spherical joints instead of rigid joints to provide several degrees of freedom for storage and deployment. These types of structures are widely applied in space, such as 17 m deployable truss antennas used in Japanese engineering test satellite Ⅷ[17], American able deployable articulated mast(ADAM) used to support inverse synthetic aperture radar in shuttle radar topographic mission[18], and folding articulated square truss(FAST)mast used to support the flexible solar arrays in ISS[19], ADAM and FAST are shown in Fig. 2. There are hundreds of joints used to connect struts or modules in these articulated truss structures.

(a) ADAM (b) FAST

Fig. 2. Articulated deployable truss structure

The main feature of these deployable structures is that joints are used to realize the structural retraction and deployment. The number of the joints used in the deployable structures vary from several to hundreds dependants on the different scale of the structures. Although hundreds of joints contained in larger space deployable structures, these joint dominated structures are still primary choice for large scale or high precision

deployment and support structures due to their high stiffness and advantageous perfermence[20]. But models of these jointed structures must be accurately established, and effects of joint on system performance must be deeply understood and analyzed before these structures are applied in missions. The following sections will discuss joint linear and nonlinear effects on dynamics of the jointed systems.

3 Joint Linear Effects Analysis

3.1 Modeling of jointed system

The space deployable structures usually extend from the spacecraft, the top end is used to support the apparatus, while the root end is fixed on the spacecraft. So the deployable structure can be modeled as cantilever beam containing joints. As shown in Fig. 3, a simple model is a cantilever beam system of two identical beams connected by one joint. The folded state length of the structure will be shorter as the number of joints increasing, so the more joints used, the higher of structural packaging efficiency.

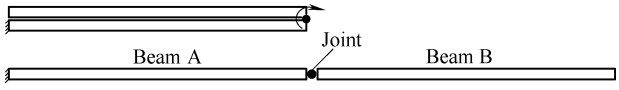

Fig. 3. Jointed cantilever beam(Folded and Deployed)

To analyze the joint effects, finite element method is used to establish the motion equation of the above jointed system. Each beam is represented by four beam elements, and each beam element has 4-DOF with translation and rotation allowed at each end, considering the two DOFs at the end of beam are restricted, there are totally 17 DOFs as shown in Fig. 4.

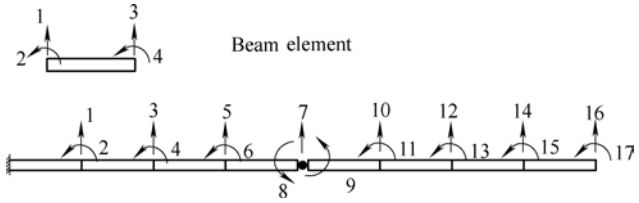

Fig. 4. Finite element model of jointed cantilever beam

The stiffness and mass matrices of the beam element are

$$\boldsymbol{k}_{\mathrm{e}}=\frac{EI}{l_{\mathrm{e}}^{3}}\begin{pmatrix}12 & 6l_{\mathrm{e}} & -12 & 6l_{\mathrm{e}}\\ 6l_{\mathrm{e}} & 4l_{\mathrm{e}}^{2} & -6l_{\mathrm{e}} & 2l_{\mathrm{e}}^{2}\\ -12 & -6l_{\mathrm{e}} & 12 & -6l_{\mathrm{e}}\\ 6l_{\mathrm{e}} & 2l_{\mathrm{e}}^{2} & -6l_{\mathrm{e}} & 4l_{\mathrm{e}}^{2}\end{pmatrix}, \tag{1}$$

and

$$\boldsymbol{m}_{\mathrm{e}}=\frac{\rho l_{\mathrm{e}}}{420}\begin{pmatrix}156 & 22l_{\mathrm{e}} & 54 & -13l_{\mathrm{e}}\\ 22l_{\mathrm{e}} & 4l_{\mathrm{e}}^{2} & 13l_{\mathrm{e}} & -3l_{\mathrm{e}}^{2}\\ 54 & 13l_{\mathrm{e}} & 156 & -22l_{\mathrm{e}}\\ -13l_{\mathrm{e}} & -3l_{\mathrm{e}}^{2} & -22l_{\mathrm{e}} & 4l_{\mathrm{e}}^{2}\end{pmatrix}, \tag{2}$$

where EI is stiffness of beam cross-sectional, l_{e} is length of element, ρ is mass of per unit length of beam.

If the joint stiffness is assumed as k_{j}, then the system stiffness and mass matrices can be obtained by assembling the stiffness and mass matrices of these beam elements and adding the joint stiffness to stiffness matrix at corresponding joint location, they are respectively $\boldsymbol{K}_{17\times17}$ and $\boldsymbol{M}_{17\times17}$.

Firstly, the system damping is not considered, so the system motion equation can be expressed as

$$\boldsymbol{M}\ddot{q}+\boldsymbol{K}q=\boldsymbol{F}. \tag{3}$$

The modal solution of Eq. (3) is a straightforward eigenvalue problem, the eigenvalues delegate system modal frequencies, while the eigenvectors delegate system modal shapes.

3.2 Effects of joint stiffness

The length of the cantilever beam is assumed as 8 m，modulus of elasticity is E=70 GPa，beam section bending stiffness is assumed as EI=343.6 kN • m^2. When the joint is located at the middle of the beam, the frequencies of the cantilever beam with different joint stiffness are calculated and given in Table 1. Frequencies of the same cantilever beam without joint(delegated by CON) are also calculated and compared with frequencies of jointed beam. The mode shapes are compared graphically in Fig. 5.

Table 1. Frequencies of cantilever beam with different joint stiffness and continuous beam Hz

Mode No.	1	2	3	4	5	6	7	8
$k_{\mathrm{j}}=0.1EI/l_{\mathrm{e}}$	0.879 3	4.313 8	19.536 9	29.858 9	63.632 2	80.522 9	134.618 4	156.702 7
$k_{\mathrm{j}}=EI/l_{\mathrm{e}}$	1.082 1	6.258 4	19.540 8	35.035 6	63.632 3	88.268 5	134.620 7	166.182 7
$k_{\mathrm{j}}=10EI/l_{\mathrm{e}}$	1.109 8	6.888 9	19.542 1	37.896 1	63.632 3	94.471 7	134.622 3	176.545 1
CON	1.113 0	6.975 7	19.542 3	38.357 7	63.632 3	95.632 5	134.622 6	178.844 1

It is clearly shown in Fig. 5 that when the peak shapes occur at the location of the joint, the peak shapes become the cusp shapes due to bending stiffness decreases suddenly at the joint location(modes 1, 2, 4, 6, 8), and the less of the joint stiffness, the sharper of the cusp shapes. But when the peak shapes do not occur at the location of joint(modes 3, 5, 7), difference of the mode shapes are not distinct. Mode frequencies comparison of the cantilever beam with different joint stiffness are clearly shown in Fig. 6, the frequencies of modes 1, 2, 4, 6, 8 increase distinctly as the

joint stiffness increasing, while the frequencies of modes 3, 5, 7 have little change. Presence of joint in the system reduces system natural frequencies, but effects of joint stiffness on natural frequencies of different modes are different.

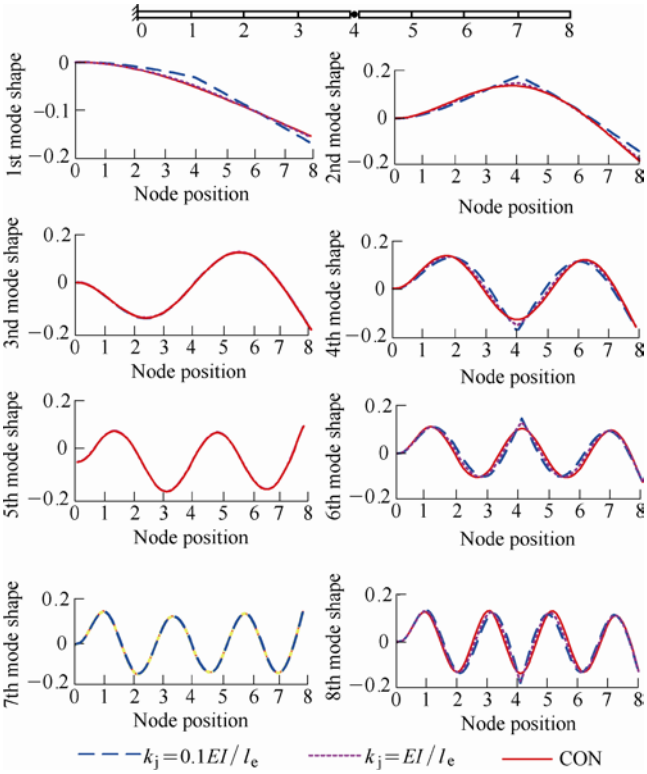

Fig. 5.　Mode shapes of cantilever beam with different joint stiffness and continuous beam

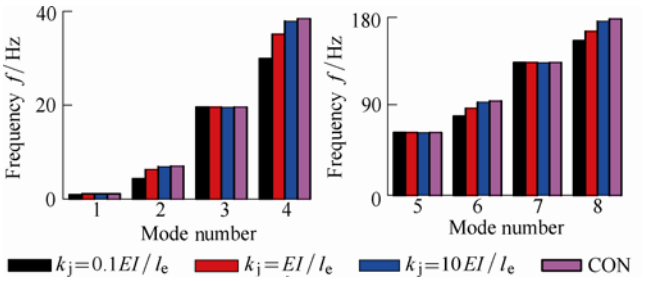

Fig. 6.　Frequencies comparison of beam with different joint stiffness

The joint stiffness has significant effect on local mode frequencies and mode shapes at location of joint. As shown in Table 2 and Fig. 7, the joint local frequencies increase and the corresponding mode shapes become shaper near the joint location and smoother far away from the joint location as the joint stiffness increasing.

Table 2.　Local frequencies under different joint stiffness

Joint stiffness k_j/(N • m • rad^{-1})	$k_j=0.1EI/l_e$	$k_j=EI/l_e$	$k_j=10EI/l_e$
Frequency f/Hz	1 259.42	1 421.08	2 749.75

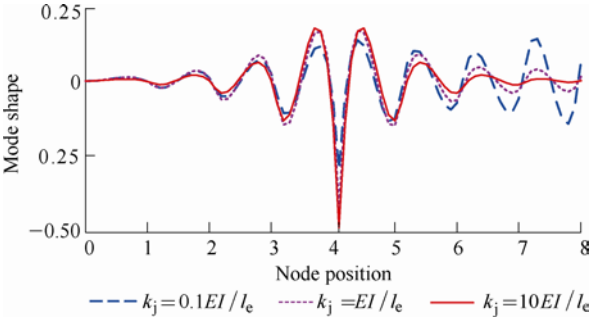

Fig. 7.　Local mode shapes under different joint stiffness

3.3　Effect of joint location

To analyze effects of joint location on natural frequencies and mode shapes of the jointed system, joint is placed near the top end and near the root end of the cantilever beam respectively. Mode shapes and frequencies comparison of the jointed beam with different joint stiffness are shown in Fig. 8 and Fig. 9.

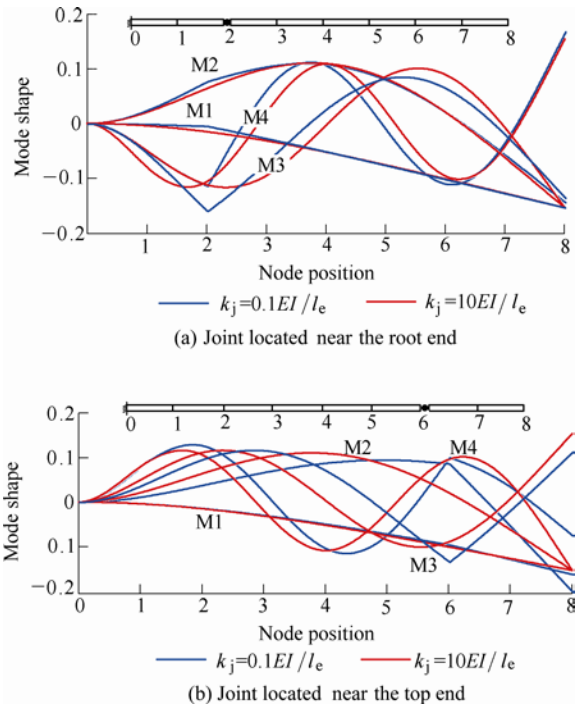

Fig. 8.　Mode shapes of jointed beam with different joint location

Frequencies have the same vary trend which increase with joint stiffness increasing, but the difference from the joint placed in the middle of the beam is that joint has effects on each mode frequency whenever the joint placed near the top end or near the root end, that is because the joint participates in each vibration mode, and the cusp shapes occurs at the location of joint in each mode shape.

The natural frequencies of the cantilever beam system with the joint placed at different location are further compared when the joint stiffness k_j is $0.1EI/l_e$, as shown in Fig. 10.　When the joint stiffness is same, location of the joint significantly affects frequencies of the jointed system. The first natural frequency is highest when the joint is near

the top end while it is lowest when the joint is near the root end. The natural frequencies of other modes vary with the relationship of the peak shapes and joint location. When the location of peak shapes are at the location of the joint or nearest to the joint location, the natural frequency is the lowest. It is noted that the peak shapes of mode 5 do not occur at the any joint location, so the natural frequency are affected less by the joint. The system frequencies with wherever the joint placed are all lower than that of continuous beam due to the joint makes the system more flexible and thereby reduces the overall stiffness in all modes.

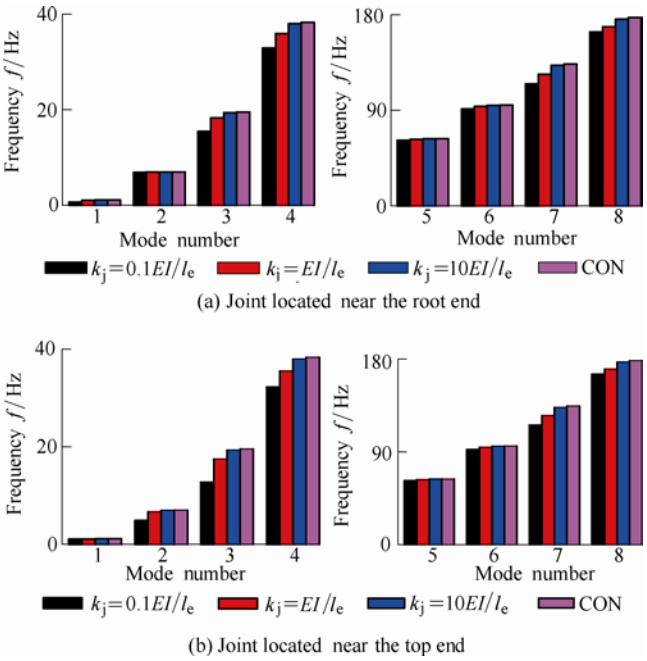

Fig. 9. Frequencies comparison of jointed beam with different joint stiffness

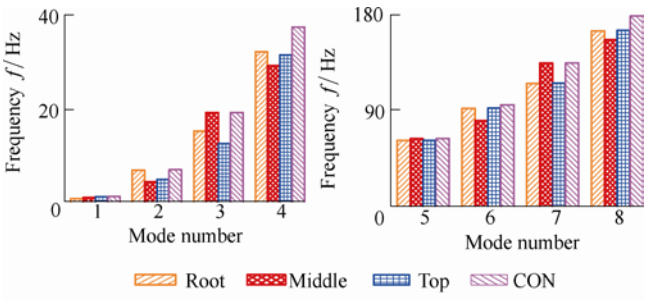

Fig. 10. Frequencies comparison of jointed beam with different joint location(k_j=0.1EI/l_e)

3.4 Effect of joint numbers

In space deployable structures, the more joints are used means that the higher packaging efficiency can be achieved. But the more joints are used, the more complex and instable of the system. The same simple jointed cantilever beam model with different numbers of joints is used to analyze how the joint numbers affect the frequencies and mode shapes of the jointed system. The frequencies and mode shapes of the same beam connected with two joints and three joints are calculated by solving the system equation of motion. All joints are assumed identical in the same analysis model. Fig. 11 shows the comparison of mode shapes and natural frequencies of the cantilever beam with two joints, two joints have more influence on the mode shapes and natural frequencies than one joint, especially the higher mode shapes are affected significantly by the joint near the root end of the beam.

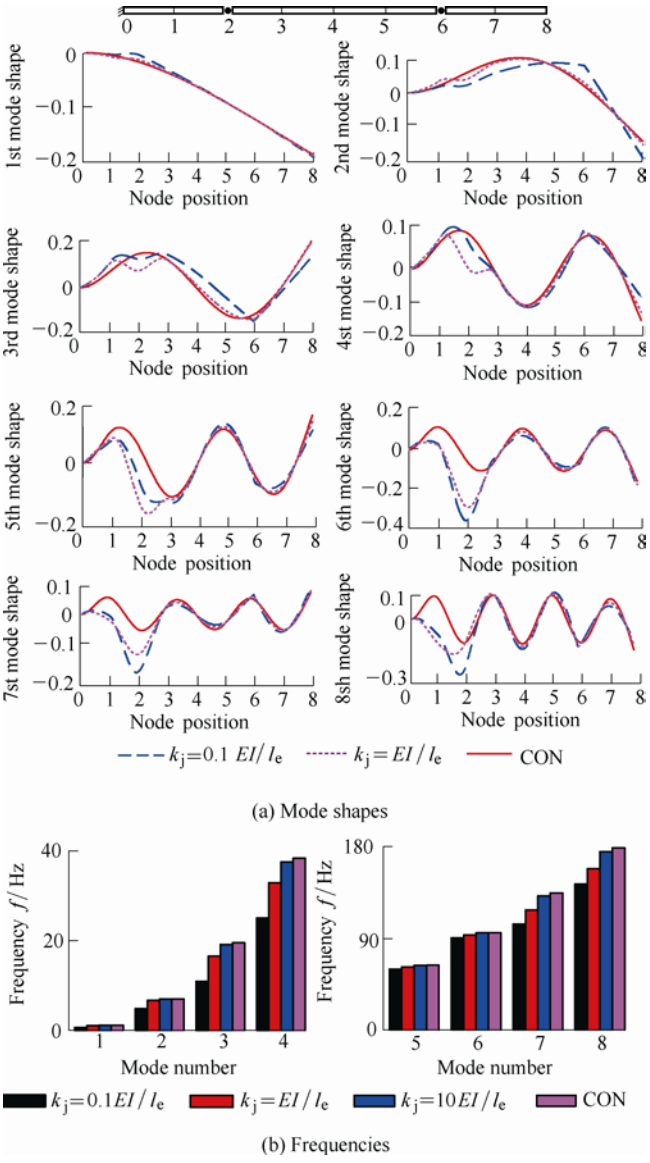

Fig. 11. Mode shapes and frequencies comparison of jointed beam with two joints

The mode shapes and natural frequencies of the cantilever beam with three joints are compared and shown in Fig. 12, cusp shapes occur when location of peak shapes and the locations of the joint are same. The more cusp shapes occur, the more natural frequencies are influenced by the joints. Three peak shapes of mode 4 and mode 8 occur at three locations of joints, so there are three cusp shapes occur, and these mode frequencies are affected more

significantly by the joints.

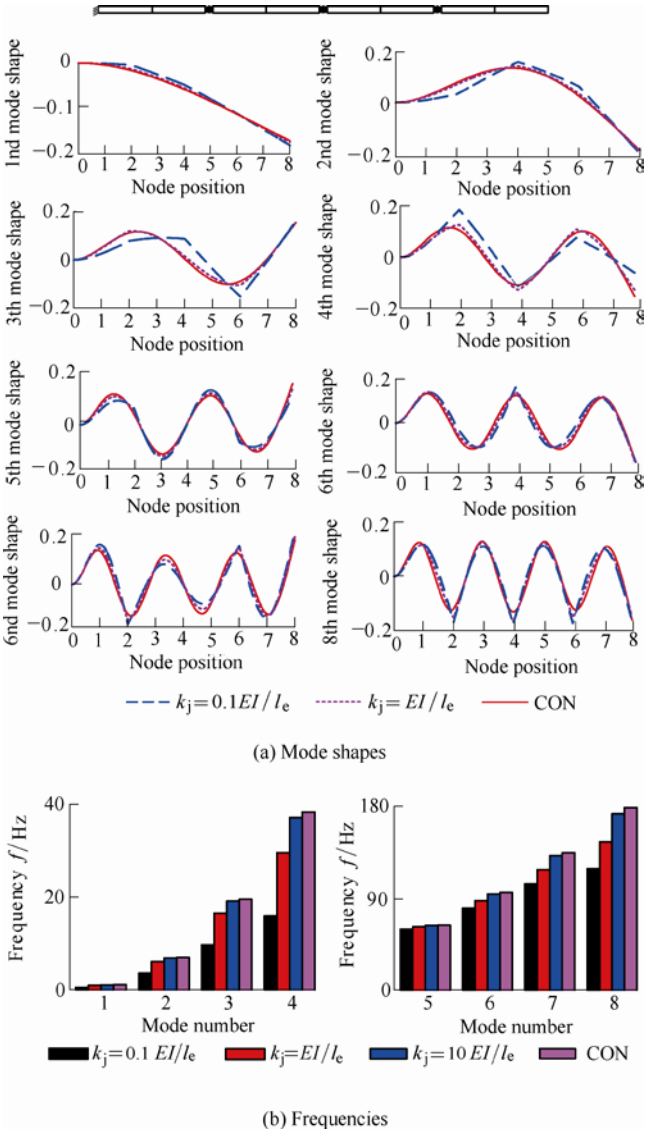

Fig. 12. Mode shapes and frequencies comparison of jointed beam with three joints

The influence of the joint number on the natural frequencies of the system are compared when the joint stiffness k_j is $0.1EI/l_e$, as shown in Fig. 13. The overall trend of the frequencies is decreasing with the joint numbers increasing, but the frequencies of mode 2 and mode 6 of the two joints system are higher than the one joint system, that is because of that the peak shapes of mode 2 and mode 6 in one joint system occur at the locations of joint, the joint participates in the vibration mode effectively, so the joint has more influence on frequencies in single joint system. The influence of the joint number on the mode shapes and frequencies also depend on the joint stiffness, it has more effect when the joint stiffness is lower. Thus it is concluded that it is not necessary that the more joints contained in the jointed system, the more influence on dynamic of the system. The effect extent of joint number on dynamic of jointed system is dependent on the practical number of joints participating in vibration mode. So effects of joint can be reduced by designing the locations of joints and avoiding the peak shapes of mode shapes to occur at the locations of joints.

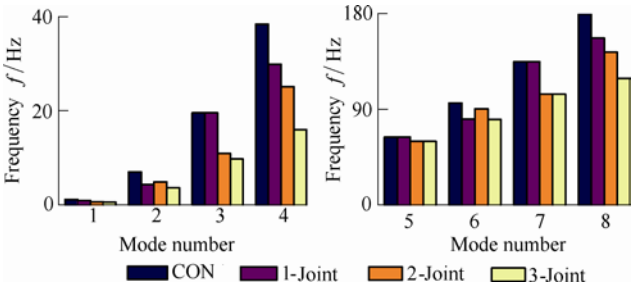

Fig. 13. Frequencies comparison of jointed beam with different number of joints (k_j=0.1EI/l_e)

3.5 Effect of joint damping

Damping in the joint is one of the most significant source of passive damping for large space deployable structures. To understand the effect of joint damping on dynamics of jointed space deployable structures, the dynamics of above jointed cantilever beam considering joint damping is investigated. Only the joint damping is considered and assumed as c_j, so the elements of damping matrix $\boldsymbol{C}$ of the jointed system are only related to joint damping c_j, the elements at the corresponding location of joint are contributed by joint damping and the elements of non-joint location are all set to be zero.

The jointed system motion equation considering damping can be expressed as

$$\boldsymbol{M}\ddot{q}+\boldsymbol{C}\dot{q}+\boldsymbol{K}q=\boldsymbol{F}, \tag{4}$$

which can be rewritten as

$$\dot{\boldsymbol{x}}=\boldsymbol{A}x-\boldsymbol{B}, \tag{5}$$

where $\boldsymbol{x}=\begin{pmatrix} q \\ \dot{q} \end{pmatrix}$,

$$\boldsymbol{A}=\begin{pmatrix} 0 & \boldsymbol{E} \\ -\boldsymbol{M}^{-1}\boldsymbol{K} & -\boldsymbol{M}^{-1}\boldsymbol{C} \end{pmatrix},$$

$$\boldsymbol{B}=\begin{pmatrix} 0 \\ -\boldsymbol{M}^{-1}\boldsymbol{F} \end{pmatrix}.$$

The natural frequencies and mode shapes of the jointed system can be obtained from eigenvalues and eigenvectors by solving the characteristic equation $\dot{\boldsymbol{x}}=\boldsymbol{A}\boldsymbol{x}$.

The solved eigenvectors can be expressed as following

form:

$$x=\begin{pmatrix} q \\ \dot{q} \end{pmatrix}=\begin{pmatrix} \psi \\ \lambda\psi \end{pmatrix}, \tag{6}$$

where ψ delegates the displacements of nodal vibration, and $\lambda\psi$ delegates the velocities of nodal vibration, λ is the corresponding eigenvalues, which can be expressed as $\lambda=\alpha+\mathrm{i}\omega$, The imaginary parts of eigenvalue λ delegate the mode frequencies.

The part of eigenvector ψ can be interpreted as a mode shape, which is a time dependent mode shape because ψ is a complex vector, so unlike standard undamped modal vibrations, the mode shape of damped system changes its spatial distribution and magnitude during each cycle.

The mode shape can be expressed as

$$V=\exp(\alpha t)(\psi_{\mathrm{R}}\cos\omega t-\psi_{\mathrm{I}}\sin\omega t), \tag{7}$$

where ψ_{R} is the real part of ψ, and ψ_{I} is the imaginary part of ψ.

Take cantilever beam with three joints as example, when the joint stiffness and joint damping are assumed as $k_{\mathrm{j}}=0.1EI/l_{\mathrm{e}}$ and $c_{\mathrm{j}}=10$ respectively，solving the equation of motion and obtaining the frequencies and mode shapes of the system which are given in Table 3 and Fig. 14.

Table 3. Frequencies of cantilever beam considering joint damping Hz

Mode No.	1	2	3	4	5	6	7	8
λ	–0.000 2+ 0.569 9i	–0.008 2+ 3.598 9i	–0.057 9+ 9.735 7i	–0.109 6+ 15.973 6i	–0.068 7+ 59.690 6i	–0.228 3+ 80.414 4i	–0.528 9+ 104.088 7i	–1.113 9+ 118.893 0i

The real and imaginary parts of the mode shapes(modes 1, 2, 3, 8) are illustrated separately in Fig. 14. It is noted that the real part of the mode shapes are consistent with mode shapes of the undamped system, while the imaginary parts have more complicated shapes.

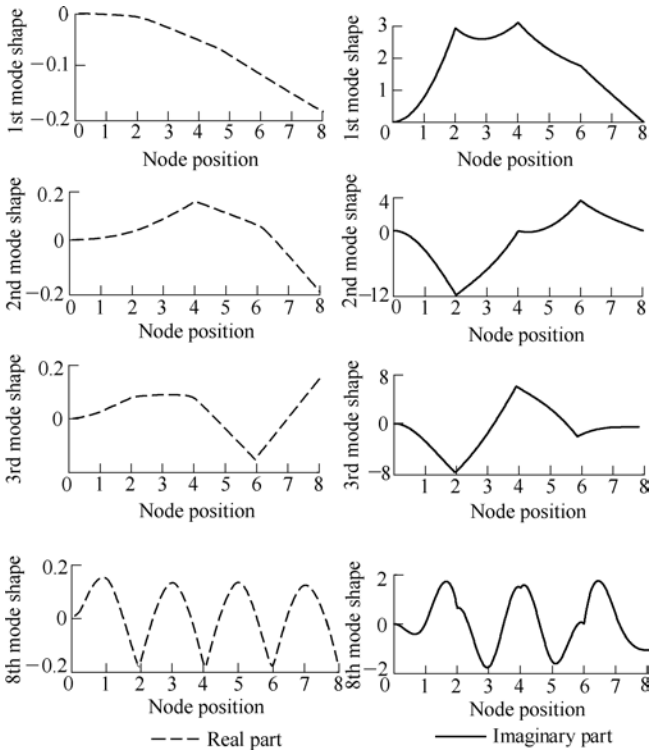

Fig. 14. Mode shapes of cantilever beam considering joint damping

To better illustrate the effect of joint damping on system modal vibration, the mode shapes time variation of mode 1 and mode 8 over the course of a vibration cycle are shown in Fig. 15. Comparing with the undamped vibration, the most prominent difference is that the mode shape does not become zero at the quarter cycle point($\omega t=\pi/2$), contrarily it is the imaginary part of the eigenvector.

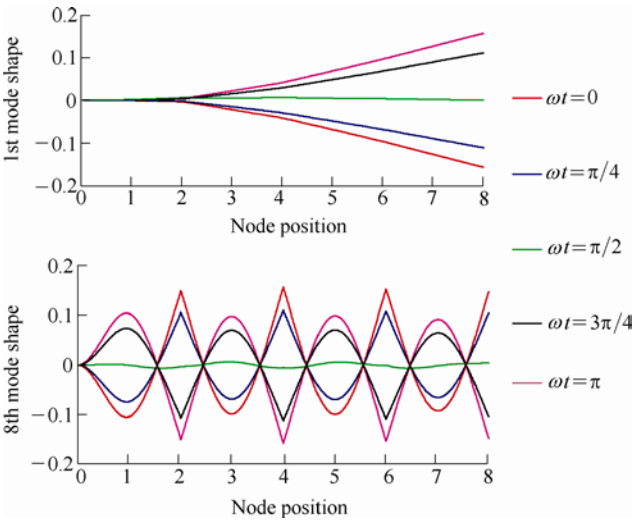

Fig. 15. Complex mode

Each eigenvalue of motion equation consists of a system resonant frequency and corresponding modal damping. The real and imaginary parts of eigenvalue vary with joint stiffness and joint damping. The variation of the first three eigenvalues with the joint damping increasing is plotted in the complex plane as shown in Fig. 16. The joint stiffness value k_{j} is fixed at $0.1EI/l_{\mathrm{e}}$, while the joint damping varies from zero to infinity, the imaginary parts of eigenvalue delegate the resonant frequencies which vary from jointed system frequency ω_{i} to continuous beam frequency ω_{c}. The real parts of the eigenvalues delegate the system modal damping whose absolute values increase firstly and then decrease. It means there is a maximum amount of modal damping achievable for each mode and the maximum amount of modal damping occurs at different values of joint damping for each mode with the given joint stiffness k_{j}.

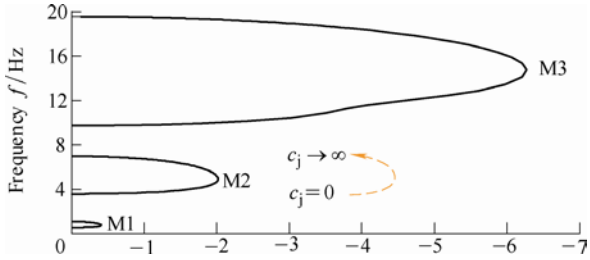

Fig. 16. Eigenvalues plotted in complex plane (k_j=0.1EI/l_e)

As shown in Fig. 17, variation of the first three eigenvalues with the joint damping increasing under the different joint stiffness k_j is compared and plotted. The values of joint stiffness are 0.1EI/l_e, EI/l_e and 10EI/l_e respectively, as the joint damping approaches infinity, the imaginary parts of eigenvalues are up to ω_c, but they start at different undamped frequencies under different joint stiffness. The comparison of the eigenvalues with different joint stiffness shows that the higher the joint stiffness, the lower the maximum modal damping achieves.

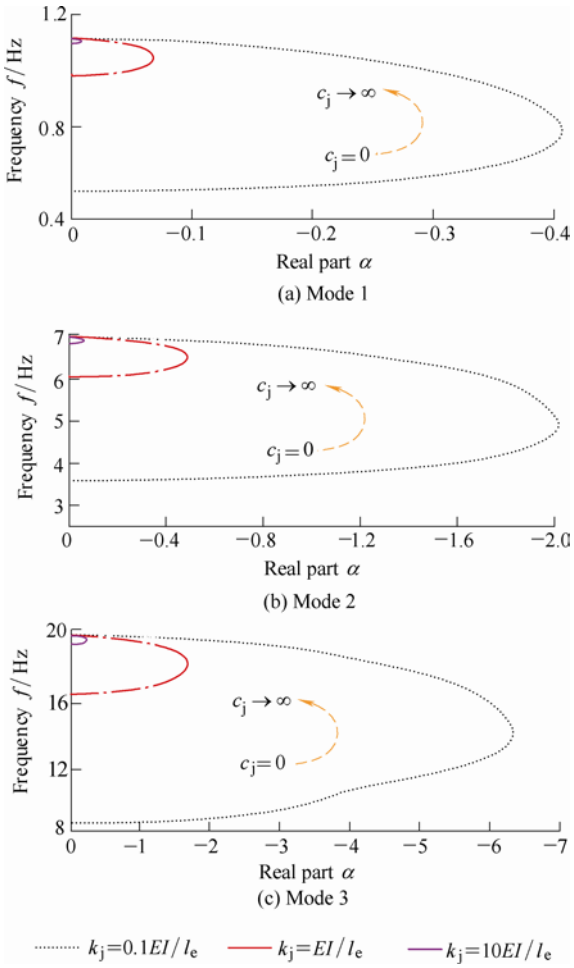

Fig. 17. Variation of eigenvalues under different joint stiffness

The joint damping needed to reach the peak modal damping and corresponding eigenvalues are calculated in Table 4. More joint damping is needed to reach the peak modal damping when joint stiffness is higher, while less joint damping is needed for higher mode with the same joint stiffness. This reflects that less joints are excited when the joints are stiffer or in a lower mode, so more joint damping is required to achieve maximum modal damping.

Table 4. Joint damping needed to reach the peak modal damping and corresponding eigenvalues

Mode No.		1	2	3
k_j=0.1EI/l_e	c_j	15 200	2 700	1 600
	λ	–0.404 2+ 0.785 7i	–2.011 2+ 4.954 6i	–6.264 7+ 14.747 3i
k_j=EI/l_e	c_j	62 700	11 100	4 160
	λ	–0.068 7+ 1.048 6i	–0.489 7+ 6.517 9i	–1.664 5+ 18.006 0i
k_j=10EI/l_e	c_j	505 000	84 800	29 500
	λ	–0.007 7+ 1.105 4i	–0.059 6+ 6.918 6i	–0.205 4+ 19.339 3i

As shown in Fig. 18, variation of eigenvalues of higher modes are compared, the mode 4 and mode 6 achieve larger modal damping compared with other modes, while the modal damping of mode 5 is not becoming larger as the mode increasing. It is shown in mode shapes of beam with three joints that there are three peak shapes occur at the locations of joint and one peak shape occurs at the location of joint respectively when the modes are 4 and 6, but there is no peak shape occurs at the location of joint when mode is 5. So it is concluded that the more joints involved or excited in the vibration, the more modal damping contributed by the joints.

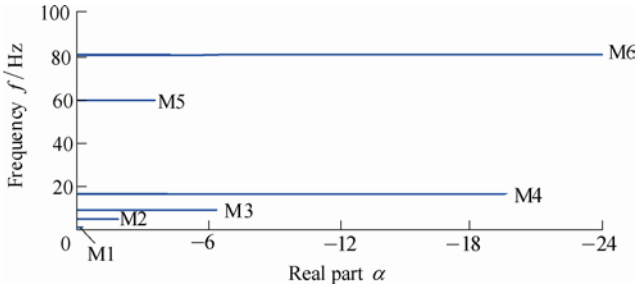

Fig. 18. Variation of eigenvalues (k_j=0.1EI/l_e)

4 Effect of Joint Nonlinearities Analysis

4.1 Joint nonlinearities description

Joints used in the space deployable structures, either pin-joints or spherical joints, not only have linear effect on dynamics of jointed system, but also have nonlinear effects due to joints present nonlinear force-displacement relationship. But the force-displacement responses are different due to different construction of joint, and the nonlinearities in the same kind of joint are also different because of different load paths or whether restricted by latches or preload. Two main nonlinear force-displacement responses may happen during deployable structures deployment process or deployed as shown in Fig. 19.

Fig. 19(a) shows nonlinear force-displacement of freeplay due to clearances between two components of the joint. The freeplay nonlinearity is characterized by two

parameters, gap dimension δ and stiffness K_{FP} beyond the gap:

$$\begin{cases} F = 0, & -\delta < q < \delta, \\ F = K_{FP}(q \mp \delta), & q > \delta \text{ or } q < -\delta. \end{cases} \tag{8}$$

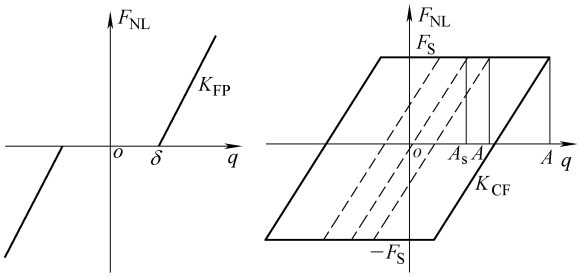

(a) Freeplay (b) Hysteresis

Fig. 19. Two main nonlinear force-displacement relationship

Fig. 19(b) shows hysteresis nonlinearity of the joint due to friction between the joint components. The characterizing parameters are slipping force F_s and stiffness K_{CF} before slip happens. Assume $A_s = F_s / K_{CF}$ and $2A_s > A$,

$$\begin{cases} F = K_{CF}(A+q) - F_S, & 0 < q < 2A_S - A, \\ F = F_S, & 2A_S - A < q < A, \\ F = F_S - K_{CF}(A-q), & q : A \to 0, \end{cases} \tag{9a}$$

or when $2A_s < A$,

$$\begin{cases} F = F_S, & 0 < q < A, \\ F = F_S - K_{CF}(A-q), & q : A \to A - 2A_S, \\ F = -F_S, & q : A - 2A_S \to 0. \end{cases} \tag{9b}$$

Due to the symmetry, the force has inverse value when $q<0$.

The describing function formulation is used in describing joint nonlinear force by calculating the first harmonic in a Fourier series expansion of the nonlinear joint force and ignoring the higher harmonics[10].

The joint nonlinear force-displacement relationship can be expressed as

$$F_{NL} = f(q,\ \dot{q}). \tag{10a}$$

Using describing function method, the nonlinear force-displacement relationship is approximated as

$$F_{NL} = f(q, \dot{q}) \approx c_p(A,\omega)q + c_q(A,\omega)\dot{q}. \tag{10b}$$

If it is assumed to be harmonic motion, $q = A\sin\omega t$, c_p, c_q are describing function coefficients, they are depend on amplitude and frequency, they are

$$c_p = \frac{1}{\pi A}\int_0^{2\pi} f(A\sin\varphi, A\omega\cos\varphi)\sin\varphi \mathrm{d}\varphi,$$

$$c_q = \frac{1}{\pi\omega A}\int_0^{2\pi} f(A\sin\varphi, A\omega\cos\varphi)\cos\varphi \mathrm{d}\varphi,$$

c_p and c_q represent equivalent stiffness and damping of joint used in the deployable truss structures respectively. For more general form of the assumed response, $q = a\sin\omega t + b\cos\omega t$, $A = \sqrt{a^2 + b^2}$, then the same describing function representation can be applied.

So the nonlinear joint force of freeplay and hysteresis are described as

$$F_{FP} = \frac{K_{FP}}{\pi}(\pi - 2\phi_1 + \sin 2\phi_1)q, \quad \phi_1 = \arcsin\frac{\delta}{A}. \tag{11}$$

$$F_{HY} = \frac{k_{CF}}{\pi}\left[\frac{\pi}{2} + \phi_1 - \frac{\sin 2\phi_1}{2} + 2\left(\frac{2}{\beta} - 1\right)\cos\phi_1\right]q + \frac{4k_{CF}}{\pi}\frac{1}{\beta}\left(1 - \frac{1}{\beta}\right)\dot{q},$$

$$\beta = \frac{A}{F_S / K_{CF}} \quad \phi_1 = \arcsin\left(\frac{2}{\beta} - 1\right). \tag{12}$$

Describing function coefficients are function of amplitude and corresponding characterizing parameters. Only the hysteresis nonlinearity contributes damping due to dissipation occurs when there is slipping.

4.2 Joint characteristics analysis

In order to further analyze the effects of joint nonlinearities on jointed system, the dynamics of one-DOF jointed system is studied in this section.

The dynamic equation of one-DOF system with nonlinear joint can be written as

$$M\ddot{q} + C\dot{q} + Kq + F_{NL} = F, \tag{13}$$

where M, C, K are linear mass, damping and stiffness respectively, F_{NL} is the nonlinear force produced by nonlinear joint which is described by Eq. (10b), F is harmonic exciting force, $F = F_0\sin\omega t$.

Assume the dynamic response is

$$q = a\sin\omega t + b\cos\omega t, \tag{14}$$

if insert the expression q and Eq. (10b) into Eq. (13), and divided by sine and cosine terms, two new equations are obtained:

$$(-M\omega^2 + K + c_p)a - (C\omega + c_q\omega)b = F_0, \tag{15a}$$

$$(-M\omega^2 + K + c_p)b + (C\omega + c_q\omega)a = 0. \tag{15b}$$

From above two equations, the dynamic respond amplitude can be derived:

$$A=\frac{\tilde{F}}{\sqrt{(1-\Omega^2+\tilde{c}_{\mathrm{p}})^2+(2\zeta\Omega+\tilde{c}_{\mathrm{q}}\Omega)^2}}, \tag{16}$$

where $\omega_0=\sqrt{K/M}$, $\zeta=C/(2\sqrt{KM})$, $\Omega=\omega/\omega_0$, $\tilde{c}_{\mathrm{p}}=c_{\mathrm{p}}/K$, $\tilde{c}_{\mathrm{q}}=c_{\mathrm{q}}\omega_0/K$ and $\tilde{F}=F_0/K$.

So Eq. (16) is the forced response of one-DOF system with nonlinear joint. It is clearly found that $\tilde{c}_{\mathrm{p}}$ and $\tilde{c}_{\mathrm{q}}$ are stiffness and damping contributed by joint to the system respectively.

If no damping is considered and the exciting force is set to zero, the equations of motion become

$$1-\Omega^2+\tilde{c}_{\mathrm{p}}=0, \tag{17}$$

$\tilde{c}_{\mathrm{p}}$ is a function of amplitude A. So Eq. (17) can be converted to expression of amplitude A as function of ω. The curve A-ω represents the degree of joint nonlinearity.

The nonlinearities of joints and how the characterizing parameters affect nonlinearities are analyzed as follows. Due to the physical parameters of the system is not easy to be determined, specially K_{FP} and K_{CF} must be identified from experimental measures, so the following joint nonlinearity analysis mainly focuses on changing trend of nonlinear dynamic responses at different given parameters rather than magnitudes.

4.2.1 *Freeplay*

To keep the mobility of the links connected by joints, there is usually clearance remained between joint connect faces, and the manufacture errors also affect clearance of the joints. As shown in Fig. 20, the forced response of freeplay nonlinearity can be divided into two parts. The first part is that the amplitude is smaller than the gap in the joint ($A<\delta$) when the exciting force is at its low level, the freeplay nonlinearity does not present in the response curves. The responses are same as the linear system, the responses are around the natural frequency ω_0. However the amplitude exceed the gap in the joint ($A>\delta$), the responses change rapidly and around another frequency $\sqrt{1+K_{\mathrm{FP}}/K}\omega_0$. The backbone curve (dash dot line) defined by BOWDEN[10] describes the responses changing trend. Fig. 20(a) shows the response curves under different exciting force levels. Fig. 20(b) is the response curves with different δ, it will need larger exciting force to produce a larger amplitude to exceed the joint gap as δ increasing. Fig. 20(c) shows the responses of the system with different joint stiffness parameter K_{FP}, the nonlinearities become more distinct and the amplitudes at same exciting force lever decrease as the K_{FP} increasing.

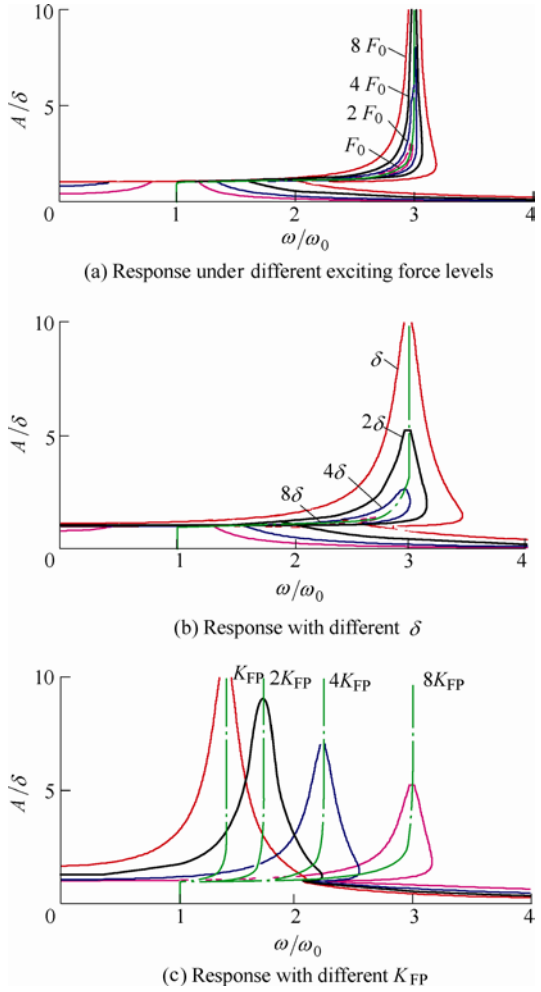

(a) Response under different exciting force levels

(b) Response with different δ

(c) Response with different K_{FP}

Fig. 20. Response of freeplay nonlinearity

4.2.2 *Hysteresis*

The responses of the hysteresis nonlinearity is similar with responses of freeplay, as shown in Fig. 21. There are also two resonance frequencies, distinguished by whether there is slipping. When the amplitude is small ($A<A_{\mathrm{S}}$), slipping does not happen, the resonance frequency is $\sqrt{1+K_{\mathrm{CF}}/K}\omega_0$. While the amplitude is larger ($A>A_{\mathrm{S}}$), slipping happens and the stiffness of the joint decreases to zero rapidly, the resonance frequency changes to ω_0. The amplitude is very sensitive to the exciting force due to stiffness contributed by joint disappears when slipping happens, as shown in Fig. 21(a). The amplitude is more sensitive to the exciting force, which increases significantly and rapidly with the exciting force increasing a small level. The larger of K_{CF}, the more nonlinear presents in the response curves. To decrease the slipping force has the same effect as to increase the exciting force as shown in Fig. 21(c).

4.3 Nonlinear dynamic test

To identify the nonlinear effect of the joints on the deployable structure, the dynamic responses of the deployable truss mast under different excitation force level

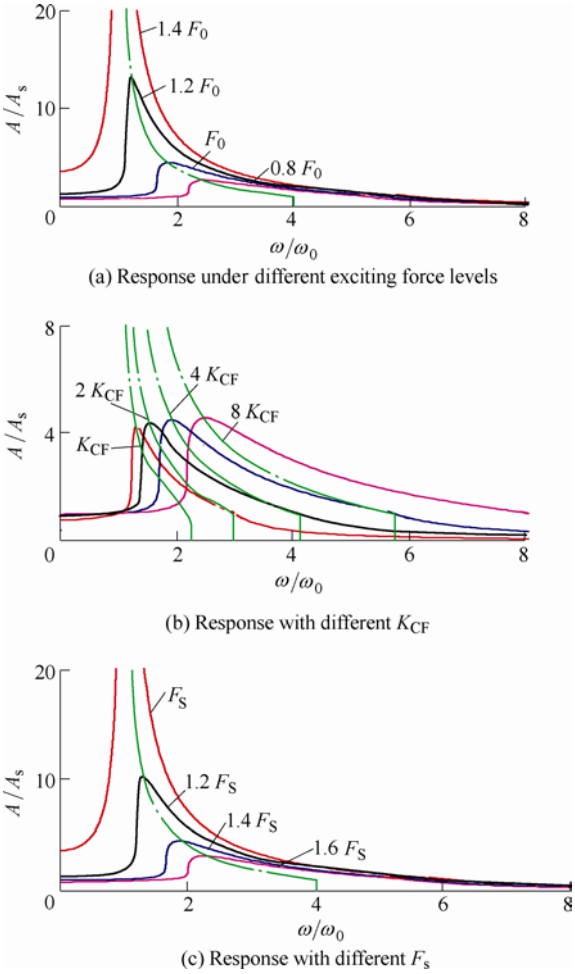

Fig. 21. Response of hysteresis nonlinearity

are measured in this section. As shown in Fig. 22 is a deployable articulated truss mast fixed on the working face of the vibration table at one end as a cantilever beam. It is a modular deployable structure which constructed by articulating basic bay repeatedly using spherical joints[21]. There are eight joints in each basic bay, and dynamic responses of the deployable truss mast contains five bays are tested in the experiment. The sine sweep vibration tests of the truss structure under different exciting force levels are tested. The dynamic responses of the truss are measured as shown in Fig. 23, the plot spans the first three model frequencies. It is similar with Fig. 21(a), the response characteristics of the structure illustrate a shift to lower resonant frequency and higher amplitude as the excitation force increasing. The finite element model of the tested truss is developed and joints are modeled as rigid connection, the natural frequencies calculated by FEM are signed by vertical dash dot line in Fig. 23, which are higher than experimental results, the comparison shows joints lower the stiffness of the truss significantly. Nonlinear dynamic behavior of the truss is mainly contributed by coulomb friction nonlinearity of the joints, the joint has fairly high stiffness when the friction mechanism is sticking at lower excitation force level, while the stiffness of the joint decreases as soon as the joint mechanism slips at higher excitation, the peak amplitude is also very strongly damped by hysteresis. So the joint nonlinear dynamic behavior in this tested structure can be modeled as coulomb friction nonlinear hysteresis.

Fig. 22. Truss vibration experiment

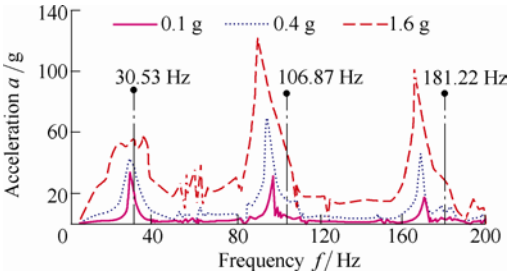

Fig. 23. Truss mast dynamic responses under different excitation force level

It is found that the joints have significant nonlinear effect on dynamic of deployable truss structure from experiment test results. Nonlinear joint behaviors present highly complex responses which are hard to model, but it is concluded from the analysis and experiment in this paper that joint nonlinearities can be represented conveniently and efficiently using describing function method. The accurate nonlinear dynamic model of the joint-dominated space deployable truss will be further researched based on combination theoretical modeling and experiment tests.

5 Conclusions

(1) The presence of joint in the jointed system can lower the natural frequency of the system, and the less of joint stiffness, the more flexible of the system.

(2) The influence degree of joint on natural frequencies and mode shapes of jointed system is dependent on the practical numbers of joint participating in vibration mode. So the effects of joint on dynamic of jointed system can be decreased by designing joint location and number to avoid peak shapes of mode shape occur at the locations of joints.

(3) There is maximum modal damping of jointed system exists at certain joint damping for each mode, and the maximum modal damping varies with joint stiffness. The higher the joint stiffness, the lower the maximum modal damping achieves, more joint damping is required to

achieve maximum modal damping when joint is stiffer or in a lower mode.

(4) The joint nonlinear effects of freeplay and hysteresis present that the dynamic responses of jointed system switch from one resonance frequency to another frequency when amplitude exceed demarcation values. The nonlinear degree of jointed system is determined by joint characterizing parameters K_{FP} and K_{CF}.

(5) Dynamic responses of the modular beam-like deployable joint-dominated truss structure under different sinusoidal exciting force levels show that the dynamic response shifts to lower frequency and higher amplitude as the exciting force level increasing. The nonlinearity of the joints is identified as hysteresis nonlinearity.

References

[1] PUIG L, BARTON A, RANDO N. A review on large deployable structures for astrophysics missions[J]. *Acta Astronautica*, 2010, 67: 12–26.

[2] KIPER G, SOYLEMEZ E. Deployable space structures[C]// *Proceedings of the 4th International Conference on Recent Advances in Space Technologies*, Istanbul, Turkey, June 11–13, 2009: 131–138.

[3] QUINN D. Modal analysis of jointed structures[J]. *Journal of Sound and Vibration*, 2012, 331(1): 81–93.

[4] LAKE M S, WARREN P A, PETERSON L D. A revolute joint with linear load-displacement response for precision deployable structures[C]// *Proceedings of 37th AIAA/ASME/ASCE/AHS/ASC Structures, Structural Dynamics, and Materials Conference*, Salt Lake City, Utah, 1996.

[5] JEON S K. *Characterization of hertzian rolling microslip in precision revolute joints for deployable space structures*[D]. Boulder: University of Colorado, 2009.

[6] LAKE M S, FUNG J, GLOSS K, et al. Experimental characterization of hysteresis in a revolute joint for precision deployable structures[C]// *Proceedings of 38th AIAA/ASME/ASCE/AHS/ASC Structures, Structural Dynamics, and Materials Conference*, Kissimmee, FL, 1997, AIAA–97–1379.

[7] DUTSON J D, FOLKMANA S L. A nonlinear finite element model of a truss using pinned joints[C]// *Proceedings of 37th AIAA/ASME/ASCE/AHS/ASC Structures, Structural Dynamics and Materials Conference and Exhibit*, Salt Lake City, UT, Reston, VA, 1996: 793–803.

[8] CRAWLEY E, O'DONNELL K. Force-state mapping identification of nonlinear joints[J]. *AIAA Journal*, 1987, 25(7): 1 003–1 010.

[9] MASTERS B P, CRAWLEY E F. Multiple degree-of-freedom force-state component identification[J]. *AIAA Journal*, 1994, 32(11): 2 276–2 285.

[10] BOWDEN M L. *Dynamics of space structures with nonlinear joints*[D]. Boston: Massachusetts Institute of Technology, 1988.

[11] WEBSTER M, VANDER V W. Modeling beam-like space trusses with nonlinear joints[C]// *Proceedings of 32nd AIAA/ASME/ASCE /AHS/ASC Structures, Structural Dynamics, and Materials Conference*, Baltimore, MD, USA, 1991: 2 745–2 754.

[12] LI T J, GUO J, CAO Y Y. Dynamic characteristics analysis of deployable space structures considering joint clearance[J]. *Acta Astronautica*, 2011, 68: 974–983.

[13] TAN G E B, PELLEGRINO S. Nonlinear vibration of cable-stiffened pantographic deployable structures[J]. *Journal of Sound and Vibration*, 2008, 314: 783–802.

[14] STOHLMAN O R, PELLEGRINO S. Shape accuracy of a joint-dominated deployable mast[C]// *Proceedings of 51st AIAA/ASME/ASCE/AHS/ASC Structures, Structural Dynamics, and Materials Conference*, Orlando, Florida, April 12–15, 2010.

[15] STOHLMAN O R, PELLEGRINO S. Effects of component properties on the accuracy of a joint-dominated deployable mast[C]// *Proceedings of 52nd AIAA/ASME/ASCE/AHS/ASC Structures, Structural Dynamics and Materials Conference*, Denver, Colorado, April 4–7, 2011.

[16] REMBALA R, OWER C. Robotic assembly and maintenance of future space stations based on the ISS mission operations experience[J]. *Acta Astronautica*, 2009, 65(7–8): 912–920.

[17] YAMADA K, TSUTSUMI Y J, YOSHIHARA M, et al. Integration and testing of large deployable reflector on ETS-VIII[C]// *Proceedings of 21st International Communications Satellite Systems Conference and Exhibit*, Yokohama, Japan, 2003: 2 217.

[18] BROWN Jr, CHARLES G, SARABANDI K, et al. Validation of the shuttle radar topography mission height data[J]. *IEEE Transactions on Geoscience and Remote Sensing*, 2005,43(8): 1 707–1 715.

[19] JOHN F S. Static stability of a three-dimensional space truss[C]// *Proceedings of the XIII Space Photovoltaic Research and Technology Conference*, NASA CP–3278, 1994.

[20] UBERTINI P, GEHRELS N, CORBETT I, et al. Future of space astronomy: a global road map for the next decades[J]. *Advances in Space Research*, 2012, 50(1): 1–55.

[21] GUO H W, LIU R Q, DENG Z Q. Dynamic modeling and analysis of cable-strut deployable articulated mast[J]. *Journal of Mechanical Engineering*, 2010, 47(9): 66–71. (in Chinese)

Biographical notes

GUO Hongwei, born in 1980, is currently a lecturer at *School of Mechanical and Electrical Engineering, Harbin Institute of Technology, China*. He received his PhD degree from *Harbin Institute of Technology, China*, in 2009. His research interests include space structure design and dynamic analysis.
Tel: +86-451-86413857; E-mail: guohw@hit.edu.cn

ZHANG Jing, born in 1985, is currently PhD candidate at *School of Mechanical and Electrical Engineering, Harbin Institute of Technology, China*. She received her master degree in *Dalian University of Technology, China*, in 2010.
E-mail: free1985216@163.com

LIU Rongqiang, born in 1965, is currently a professor at *School of Mechanical and Electrical Engineering, Harbin Institute of Technology, China*. His research interests include space deployable structures, lunar lander.
E-mail: liurq@hit.edu.cn

DENG Zongquan, born in 1956, is currently a professor at *School of Mechanical and Electrical Engineering, Harbin Institute of Technology, China*. His research interests include space structures and mechnism, lunar mobile robotics.
E-mail: denzq@hit.edu.cn